GODDARD GRANT

IN-43-CR

200058

118.

Semi-Annual Report
on NASA GRANT NAG-5887
Entitled:

REMOTE SENSING OF GLOBAL SNOWPACK ENERGY AND MASS BALANCE:

IN-SITU MEASUREMENTS ON THE SNOW OF INTERIOR AND ARCTIC ALASKA

Submitted by

Carl S. Benson
Geophysical Institute
University of Alaska
Fairbanks, Alaska 99775-0800

To:

Ms. Genevieve E. Wiseman
Grants Officer
NASA Code 280.1
Goddard Space Flight Center
Greenbelt, Maryland 20771

March, 1989

(NASA-CR-180478) REMOTE SENSING OF GLOBAL SNOWPACK ENERGY AND MASS BALANCE: IN-SITU MEASUREMENTS ON THE SNOW OF INTERIOR AND ARCTIC ALASKA Semiannual Report (Alaska Univ.) 11 p

N89-23956

Unclas

CSCL 08L G3/43 0200058

Table of Contents

1. Microwave Data 1

2. Physical Properties of, and Physical Processes Within, Arctic and Sub-Arctic Snowpacks in Relation to Passive Microwave Data from Satellites 2

3. Landsat Image for Surface Cover Assessment 3

4. The Extreme Winter of 1988-1989 5

5. Photogrammetric Control for Glacier Measurements on Landsat Images 6

6. References 7

Figures 8

This project is continuing along the lines outlined in the last semi-annual report, dated August, 1988.

1. Microwave Data

An example of microwave brightness temperatures in interior Alaska reveals several features of interest. Figure 1 shows data from six cells* in the eastern half of the Fairbanks quadrange. It shows:

- Up to three times more variability from one cell to the next in winter than in summer (5 to 15 K in winter and about 5 K in summer).
- The overall range of temperature from week to week is about seven times greater in winter than in summer. This is similar to the behavior of air temperature in the Fairbanks area where the winter range of temperature (averaged over fifty years of record) is about twice the summer range.
- The difference between microwave brightness temperature and measured surface (air) temperature is greater in winter than in summer. The microwave brightness temperature is about 25 K less than air temperature during summer but 35 to 60 K less during winter. Also, the maximum differences clearly occur during the coldest times of the winter.
- The presence of snow cover appears to contribute to increasing the difference between air temperature and brightness temperature. These relationships are shown in Figure 2 which compares brightness temperature from one of the cells in Figure 1 with air temperature and snow depth.

Considerations like these prompted us to examine the physical properties of the snow and the process which operate on it.

* The cell used in this example is larger than the one proposed in the text below; in this case it is ½ degree latitude and ½ degree longitude.

2. Physical Properties of, and Physical Processes Within, Arctic and Sub-Arctic Snowpacks in Relation to Passive Microwave Data from Satellites

Studies of snow pit data which demonstrate the upward flux of water vapor in the snow pack of interior Alaska have continued during the past winter. The existence of convection under simplified conditions has been demonstrated in the Ph.D. research of Matthew Sturm (1989). The role of this convection in vapor transport and snow metamorphism is being clarified. The importance of irregular substrate under the snow in enhancing convection needs to be studied. In the past we have concentrated on defining the physical evolution of this snow cover under idealized, undisturbed conditions with a uniform and horizontal base and no complications from vegetation. Our field work during the winter and spring of 1989 has concentrated on providing a description of the complexities of substrate. Particular attention is being paid to variations in snow cover on water surfaces, and in forested regions.

The application of passive microwave data to snow cover in Alaska was outlined in the last semi-annual report. It contained eight figures which summarized 37 GHz brightness temperatures along a North-South traverse at the 150°W meridian. The exceptionally low brightness temperatures (180 to 200°K) during winter have been attributed to structural features in the snow, especially to the growth of large depth-hoar crystals at the base of the snowpack (Hall and others, 1986). The variability of the natural snow structure complicates interpretation. This is the primary reason for our above-mentioned attention to detailed structural study of the snow in various environments.

Mature spruce forests have extremely variable snow covers because of the way the trees intercept snow as it falls. Around the base of each spruce tree there is a region with markedly reduced snow. For example, in March 1989, large spruce trees

in the Fairbanks area had "wells" of decreased snow cover on the order of 5 cm deep extending to a radius of 90 to 100 cm. Between trees the snow was 60 cm deep. However, the snow between trees was irregular because of cavities, up to 20 cm diameter (caused by bushes and irregular bent over willows, small spruce, etc.) and by lumps of snow which fall from the spruce trees (some of the lumps are icy). Smaller spruce trees have smaller *wells* around them.

Deciduous forests are less disruptive to snow cover than spruce forests. Their effect is more like that of a series of posts in the snow. They have negligible wells of decreased snow cover around them, and to a lesser extent snow falls from them to the snow cover between trees.

Many areas have mixed forests with spruce and deciduous trees present in complex patterns. At this time it appears that spruce trees produce the most complex environment. In valley bottoms, where wind is rare in the winter, new snow can remain undisturbed in spruce trees for weeks at a time because temperatures are well below the melting point and solar radiation is negligible. There is no loss by melting from this snow in the trees. Later in the winter (March) solar radiation will enhance evaporative losses. Solar radiation absorbed by the dark spruce through thin snow cover can cause localized melt and allow lumps of icy snow to drop to the snow cover on the ground. During mid-winter a wind storm can shake snow off the trees and cause the overall albedo of the forest to increase by nearly 50% in a very short period of time.

3. Landsat Image for Surface Cover Assessment

We are collaborating with the U.S. Forest Service in Anchorage to obtain suitable Landsat MSS scenes which have been classified according to surface cover. The USFS supervised classification covers the Tanana river basin and is based upon

the 4 Landsat MSS bands from imagery obtained in the mid-1970's. A total of 32 surface types were recognized.

The steps in preparing the supervised classification are:

1. Identify representative surface cover areas, or training sites — these are groups of pixels covering uniform type localities.
2. Calculate statistics for each training site, i.e., the mean vector using the 4 bands and the covariance between bands.
3. Go through entire scene assigning unknown pixels to the training site which is statistically closest to it.

The next step will be to lay a grid of $\frac{1}{4}$ degree latitude and $\frac{1}{2}$ degree longitude over the image and determine the relative proportion of various surfaces within each cell of this grid. At 65°N the grid size is: $\frac{1}{4}$ degree latitude = 27.8 km, and $\frac{1}{2}$ degree longitude = 23.5 km or 652 km^2. Each Landsat pixel is 79 m on a side or 6241 m^2 = 0.00624 km^2, so there are 10^5 pixels per grid cell.

The U.S. Forest Service subdivision into 32 types represents a finer breakdown than we require. An experiment with an image from June 6, 1976, was done in the Fairbanks quadrangle using ten surface types: ▸ snow, ▸ lakes, ▸ rivers, ▸ streams, ▸ deciduous forest, ▸ coniferous forest, ▸ mixed forest, ▸ swamp and forest-free areas, ▸ Alluvium, and ▸ bedrock. The ten subdivisions seemed adequate and may still include more detail than is necessary in our attempt to understand the influence of snow cover on mircowave emission.

The extreme types of snow cover we recognize include five overall types:

a. snow on clear open ground with negligible vegetation perforating the snow cover,
b. snow on ice surfaces of swamps, lakes, rivers or smaller streams,
c. snow in spruce forest,
d. snow in deciduous forest, and

e. snow in mixed spruce and deciduous forest.

There are subdivisions of these types. Most notably type (a) depends on wind action for the presence or absence of hard, fine-grained wind slabs and a variable amount of depth hoar depending on seasonal history, vegetation type and the amount of irregularity at the bottom.

Type (b) varies markedly because of interaction between the snow cover and the ice below — in addition to an upward flux of water vapor from the ice surface, interaction with weeds in swampy areas produces cavities and coarse depth hoar at the snow ice interface; in most small streams overflow icing produces layers of aufeis, which eliminate depth hoar.

We are working to characterize the types quantitatively for use in defining the makeup of cells for microwave data. The five overall snow cover types, with some modification as indicated above, are probably adequate for the $\frac{1}{4}$ degree latitude by $\frac{1}{2}$ degree longitude cells at 65°N. Clearly the 32 surface types defined in the Forest Service classification contains too much detail for our purpose.

4. The Extreme Winter of 1988-1989

Although winter is still in progress, there has already been significantly more than average snow cover in interior and Arctic Alaska. On the Arctic Slope this snow has also been subjected to extraordinary wind drifting. Furthermore, the months of January and February, 1989, were marked by extreme low and extreme high temperatures respectively. For example at Nome, Alaska, new all-time low temperature records were set on thirteen consecutive days in January followed in a week by four all-time high temperature records in February. Barrow set nine new low records in January and sixteen new all-time highs in February.

Microwave data from satellites obtained during the winter of 1988-1989 can be compared with these well-documented extreme conditions. This should provide

useful information in the interpretation of the microwave data sets from 1985, and before, up to the present.

5. Photogrammetric Control for Glacier Measurements on Landsat Images

The Wrangell Mountains in southcentral Alaska are covered by a 5000 km^2 ice cap. Several of its glaciers have undergone significant movement in recent years, as measured by surveying on the ground combined with aerial photogrammetry. This presents a well-calibrated site to look for changes in glacier termini on Landsat images. As a first step, satellite measurements using a September 1973 MSS scene registered to a September 1986 scene revealed the center lobes of Ahtna Glacier and MacKeith Glacier (both flow north from Mt. Wrangell) have advanced approximately 190 m during the thirteen-year period. This is consistent with the average 15 m per year advance that has been measured on the center lobe of MacKeith Glacier during this time. Chetaslina Glacier (flowing south from Mt. Wrangell) has not changed appreciably over the same period. The advance of the north-flowing glaciers is thought to be due to increased geothermal activity near the summit of Mt. Wrangell. This activity directs meltwater northward through subglacial channels (Sturm, 1983).

Photogrammetry on Mt. Wrangell is of special importance in calibrating and verifying results obtained from Landsat, because it is based on precise ground control points (11 on the rim of the summit caldera, 20 on the northeast flank and 7 on the west flank) and because changes in the volcano and its glaciers are large enough to be seen on Landsat images and well enough known to produce quantitative, calibrated results (Benson and Follett, 1986).

In 1988 a set of vertical aerial photographs was obtained over the summit of Mt. Wrangell and of the northeast flank glaciers where the termini are advancing. The 1988 vertical photos enabled us to make an orthophoto map of the northeast

flank glaciers which can be compared with similarly prepared orthophoto maps at the same scale (1:25,000) from 1957, 1977, 1979 and 1981. Measurements from these maps are being compared with surveying on the ground, up to 1981, and with paired Landsat images from 1973 to the present.

Photogrammetry of Mt. Wrangell's geothermally active summit and the glaciers radiating from it was continued in 1988. From these photos, stereographic photogrammetric models were made and cross sectioned, allowing calculation of ice volume loss due to volcanic heating in the north crater on the rim of the summit caldera. These calculations are still underway for 1987 and 1988. Unfortunately, it was not possible to obtain vertical photos over the Chetaslina Glacier in 1988. We will try again during 1989 when the summit craters are photographed for additional calculation of ice volume changes.

6. References

Benson, C S., and A.B. Follett, 1986: Application of photogrammetry to the study of volcano-glacier interactions on Mount Wrangell, Alaska. Photogrammetric Engineering and Remote Sensing, V. 52, pp. 813-827.

Hall, D.K., A.T.C. Chang and J.L. Foster, 1986: Detection of the depth-hoar layer in the snow-pack of the arctic coastal plain of Alaska, U.S.A., using satellite data. J. Glaciology, V. 32, No. 110, pp. 87-94.

Sturm, M., 1983: Comparison of glacier flow of two glacier systems on Mt. Wrangell, Alaska. M.S. Thesis, University of Alaska, Fairbanks, 186 pages.

Sturm, M, 1989: The role of thermal convection in Heat and Mass Transport in the Subarctic Snow Cover. Ph.D. Dissertation, University of Alaska, Fairbanks, April 1989, 184 pages.

37 GHZ BRIGHTNESS TEMPERATURE
EASTERN HALF OF FAIRBANKS QUADRANGLE

FIGURE 1

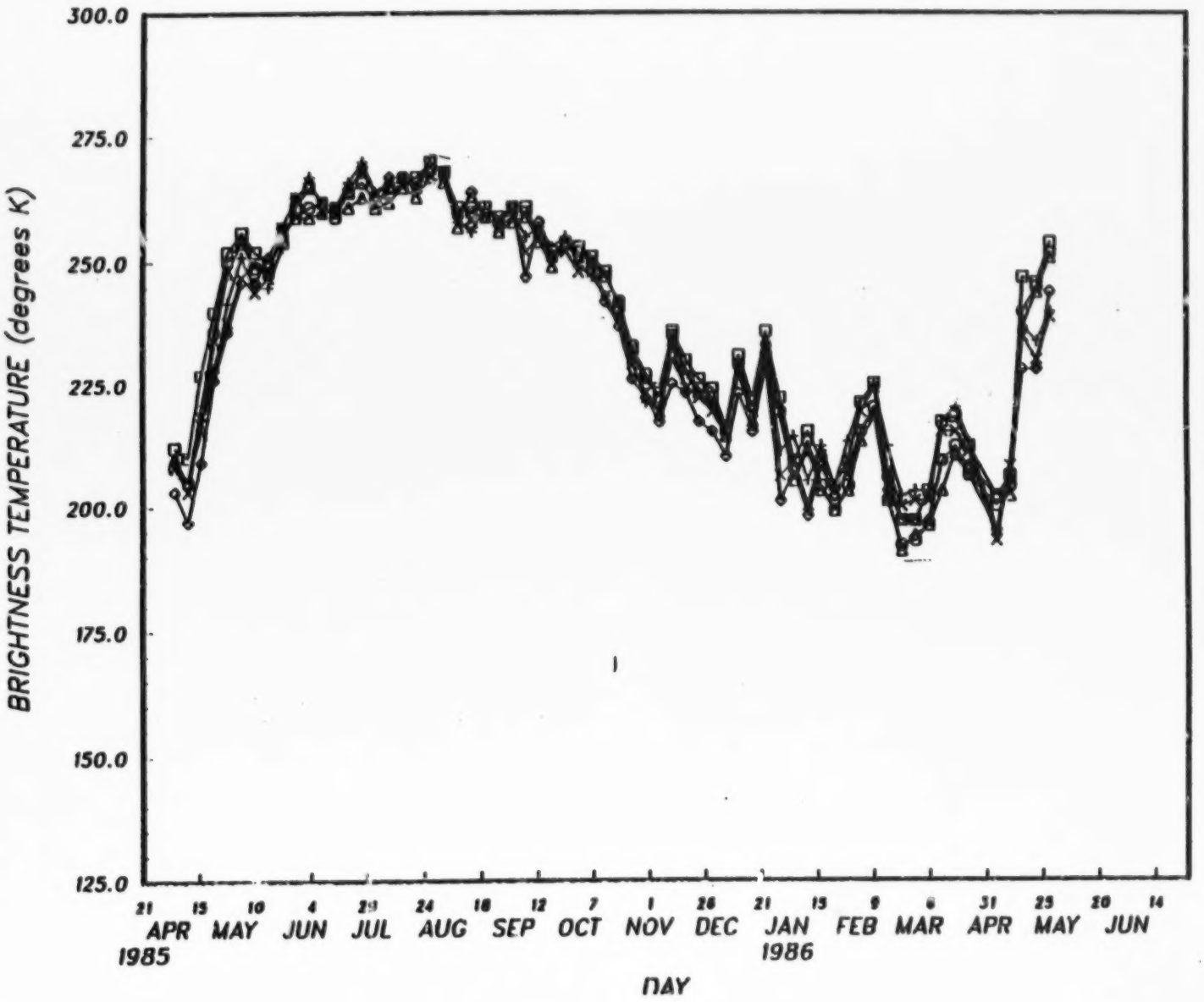

BRIGHTNESS AND AIR TEMP AND SNOW DEPTHS
EASTERN HALF OF FAIRBANKS QUADRANGLE

FIGURE 2